# Application of FY-3A/MERSI satellite data to drought monitoring in north China

**ZHU Lin, LIU Jian, ZHANG Yeping, WANG Meng**

*National Satellite Meteorological Center*, *Beijing* 100081, *China*

**Abstract:** Medium Resolution Spectral Imager (MERSI) on board the new Generation Polar-Orbiting Meteorological Satellite of China (FY-3) has five spectral channels with 250m spatial resolution, which enhances the ability to observe fine surface features and provides a new data source for drought monitoring in large area. Drought status of north China is evaluated using FY-3A/MERSI satellite data with Perpendicular Drought Index (PDI). To validate the performance of PDI in macroscale application, quantitative evaluation of drought conditions and development in Tongliao and Chifeng, two cities located in southeast of Inner Mongolia Autonomous Region of China are carried out by comparing time series drought monitoring results with field observation data. Results show that drought status derived from PDI is highly accordant with field drought observation. Satellite based PDI has significant correlation with 10cm and 20cm depth soil water content. Compared with 10cm depth soil water content, PDI has more stable relationship with 20cm depth soil water content. The drought monitoring application in this study show great potential in future drought monitoring operation using China's own satellite data.

**Key words:** FY-3A/MERSI, drought monitoring, perpendicular drought index, soil water content

**CLC number:** TP79 **Document code:** A

**Citation format:** Zhu L, Liu J, Zhang Y P and Wang M. 2010. Application of FY-3A/MERSI satellite data to drought monitoring in north China. *Journal of Remote Sensing*. **14**(5): 1004—1016

## 1 INTRODUCTION

The recent influence of global climate change, regional economic development and population growth have made drought the most frequently and severe natural disaster in China. For example, widespread and persisting drought happened in China's main winter wheat area from the winter of 2008 to the spring of 2009. In the summer of 2009, severe drought took place again in Inner Mongolia Autonomous Region, Hunan Province, Guizhou Province and Guangxi Province, with devastating impacts on local agriculture, water resources, national economies and the environment. Frequently happened drought forced scientists to seek a more effective, dynamic and feasible drought monitoring technique for better drought prevention and scientific irrigation, and even for crop yield promotion and climate change study.

During the last three decades, remote sensing technique have shown greater potential in large area applications for its high spatial resolution and regional monitoring ability compared to point-based field measurements. Indices derived from visible and near infrared bands (Kogan, 1990; Xiao *et al*., 1994; Qi *et al*., 2004; Zhan *et al*., 2007; Ghulam *et al*., 2007a,b,c), thermal infrared bands (Price, 1985; Kogan, 1995; Mcvicar & Jupp, 1998; Sandholt *et al*., 2002) and even microwave bands (Schmugge *et al*., 1986; Njoku & Li, 1999) have been widely used to capture spatial and temporal drought information near the surface. Satellite images from NOAA/AVHRR, LandsatTM, TERRA/AQUA-MODIS have been the major data sources used in China's drought applications (She & Ye, 2006). Of all these satellite sensors, data from TERRA/AQUA- MODIS has moderate spatial resolution and high spectral and temporal resolution, which is especially favorable in validation of known drought indexes and helping construct new drought index. Tan *et al*. (2004) developed an integrated drought model using MODIS based vegetation index, temperature difference between day and night, percentage of precipitation anomaly and the information of previous drought information. Song *et al*. (2004) constructed another integrated drought index using visible, near infrared and thermal infrared bands of MODIS, which is very sensitive to surface vegetation, temperature and moisture condition. Zhang *et al*. (2004) derived vegetation water content information using MODIS data and GVMI (Global Vegetation Moisture Index). They found negative relationship between vegetation water content information and regional drought condition, which is very useful for large area drought monitoring. Zhang *et al*. (2006) put forward an energy index using MODIS data, which is used to reduce the interfering of cloud to routine thermal inertia model. Qin *et al*. (2008) com-

**Received**: 2009-10-29; **Accepted**: 2010-04-18

**Foundation**: National Nature Foundation of China (No.40771148) and the Special Fund for Public Welfare Industry of China (Meteorology) (No. GYHY 200806022).

**First author biography**: ZHU Lin (1978— ), female, Assistant Researcher, E-mail: zhulin@cma.gov.cn

puted Perpendicular Drought Index (PDI) using MODIS data and apply PDI in drought monitoring application over north China. PDI is divided to several drought degrees with the reference of local soil and hydrological properties. It is demonstrated that PDI can be calculated only from red and near infrared bands which is very simple and easy to acquire. Furthermore, drought distribution from PDI is fairly accordant with real drought condition. PDI provide a simple and convenient regional drought monitoring method using MODIS data.

The development of China's new generation of polar-orbiting meteorological satellite series (FY-3) greatly enhances the surface monitoring ability of China and also provides a new data source for drought monitoring in large area. The first satellite named FY-3A of this series was successfully launched from Taiyuan in Shanxi Province at 03:02 UTC on 27 May 2008 (Yang *et al*., 2009). MERSI is one of the 11 instruments onboard this satellite, which has 5 channels with 250m spatial resolution and 15 channels with 1km resolution. MERSI has both multi-spectral and high spatial resolution properties. Compared with MODIS, FY-3A/MERSI increased 250m spatial resolution channels from 2 to 5, at the same time, MERSI includes a 250m resolution thermal infrared channel, which greatly improves the ability to observe fine surface features. Therefore, China's FY-3A/MERSI instrument has greater potential in future remote sensing applications. Further study of FY-3A/MERSI based drought monitoring technique is not only very significant for improving the using of China's own remote sensing data but also helpful for reducing the dependence of using satellite data abroad.

In this study, FY-3A/MERSI data and PDI drought index are used to monitor the drought event happened in the summer of 2009 over the northeast of Inner Mongolia Autonomous Region, China. Spatial and temporal variations of PDI are captured and the relationship between PDI and drought status is further investigated. This study is expected to provide a scientific support using China's new satellite data in operational drought monitoring work.

## 2 STUDY AREA AND DATA

### 2.1 Study area

A case study was conducted in Tongliao and Chifeng, two cities located in the main drought area of Inner Mongolia Autonomous Region, China. Its longitudes range from 116°21′E to 123°43′ E, and latitudes range from 41°17′N to 45°59′N. It is a typical arid and semi-arid region with very little precipitation (350—500 mm/a). Drought happened nearly every year in this area.

### 2.2 Data source and pre-processing

There are 20 channels in FY-3A/MERSI instrument. The third channel (Red, with central wavelength: 0.650μm, spectral band width: 0.05μm) and the fourth channel (Near infrared, with central wavelength: 0.865μm, spectral band width: 0.05μm) all have 250m spatial resolution and these two bands are very sensitive to vegetation. FY-3A/MERSI data is acquired from National Satellite Meteorological Center (NSMC) of China with HDF5 file format. They are first pre-processed by an image process software developed by NSMC so as to convert the raw data to spectral calibrated, geo-corrected and mosaicked data with 250m spatial resolution which can be directly used by ENVI. Finally, the pre-processed data are re-projected and subset to match the study area.

Soil water content measurements of 10 cm, 20 cm depth on August 8 and 18 of 2009 in the study area were collected from China Meteorological Administration (CMA). The data is sampled according to agricultural meteorological observation criterion compiled by CMA (Huang *et al*., 1993). Furthermore, drought monitoring reports for every ten days, agricultural meteorological reports, daily precipitation and temperature during the study period were also collected from Inner Mongolia weather bureau.

## 3 PERPENDICULAR DROUGHT INDEX

Fundamental study of Red and Near Infrared spectral feature space (Red-Nir space) can be traced back to 1970s. Vegetation lamina tissues can strongly absorb red spectrum and reflect near infrared spectrum. This property of vegetation can be used to construct vegetation index using red and near infrared bands so as to monitor vegetation growing. Richardson and Wiegand (1977) described Red-Nir space constructed with DNs of MSS red and near infrared bands and presented Perpendicular Vegetation Index (PVI) according to the distribution pattern of vegetation in Red-Nir space. PVI of a point in Red-Nir space is equal to the vertical length from that point to soil line. At the same time, water absorbs both red and near infrared bands strongly, so soil water content is the main factor influencing soil reflectance over red and near infrared bands. Jackson (1983) further described the distribution pattern of water in Red-Nir space. The distribution pattern of vegetation in Red-Nir space has been widely studied and applied to vegetation growth monitoring and crop yield estimation. While, the study of soil water distribution pattern in Red-Nir space is relatively less paid attention.

Zhan *et al*. (2006) and Ghulam (2006) gave a further discussion of water distribution pattern in Red-Nir space. They constructed Red-Nir space using ETM+ red band (0.630—0.690μm) and near infrared band (0.775—0.90μm). It is found that scatter plot of red and near infrared reflectance spectrum demonstrated as a typical triangle. The points at the bottom of the triangle usually correspond to bare soil points. Soil line can be captured through linear regression using these bare soil points (Richardson & Wiegand, 1977). As shown in Fig.1, points in *AD* line represent the change of vegetation cover from full cover (*A*), to partial cover (*E*) and bare soil (*D*). Not only vegetation condition, but also surface wet or dry condition can be clearly quan-

tified using this "triangle" feature space. At the soil line, points with mass water distribute near point *B*, points with moderate water content distribute at the middle of soil line, while dry points distribute near the opposite side of soil line (point *C*). As we have seen, *B*-*D*-*C* shows the direction of drought severity (Zhan *et al*., 2006).

Based on the above analysis, Ghulam (2006) developed a new drought index (Perpendicular Drought Index, PDI) using ETM+ red and near infrared bands (Fig.2). As shown in Fig.2, line *L* which is perpendicular to soil line and overpasses the origin point (0, 0) can be drawn. PDI value of any point equals to the perpendicular distance from this point to line *L*. For example, PDI value of point *E* corresponds to the length of segment *EF*.

The mathematical expression of PDI can be represented as follows (Ghulam, 2006):

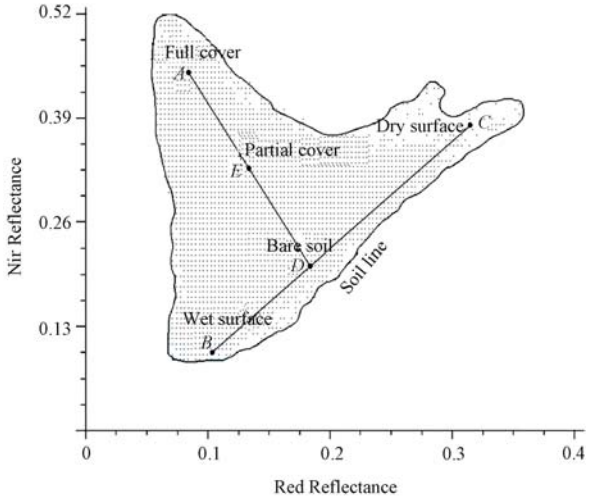


Fig. 1 Construction of Red-Nir space using ETM$^+$ data (Ghulam, 2006)

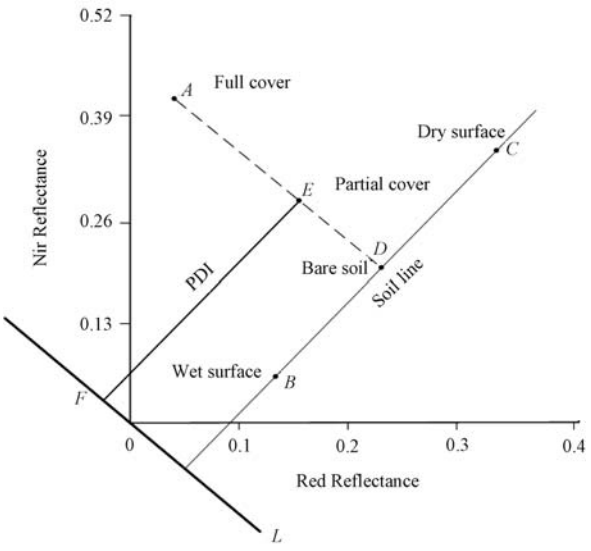


Fig. 2 Sketch map of PDI (Ghulam, 2006)

$$\mathrm{PDI}=\frac{1}{\sqrt{M^2+1}}(R_{\mathrm{red}}+MR_{\mathrm{nir}}) \quad (1)$$

where $R_{\mathrm{red}}$ and $R_{\mathrm{nir}}$ represent remote sensing data of red and near infrared bands respectively. *M* is the slope of soil line which is calculated from linear regression of bare soil points in the Red-Nir space. PDI describes the distribution pattern of soil water content in Red-Nir space. PDI ranges from 0—1. Higher PDI values represent more severe drought status and lower PDI values means the less risk of drought happened. PDI can be just acquired from Red-Nir space and the mathematical expression of PDI is also very simple. So it is very useful for monitoring regional drought status with remote sensing data.

## 4 RESULT AND ANALYSIS

Three FY-3A/MERSI images are selected to perform drought monitoring in north China. They are respectively collected on August 8, 2009, August 13, 2009 and August 20, 2009. There are two main considerations for selecting these three images: (1) It is clear and dry during this period which reduces the disturbance of cloud and atmosphere condition to a maximum degree. So the atmosphere correction and cloud detection process can be ignored. (2) There is rare precipitation and the surface temperature is higher than usual since August 1 to August 8, so the first image dated on August 8, 2009 can be a reflection of drought status in the beginning of August, 2009 of the study area. During the two periods of August 8—13, 2009 and August 12—20, 2009, there are different amounts of precipitation in the study area. Therefore the time series of images can reflect the sensitivity of FY-3A/MERSI data to drought dynamics. The calculation of *M* is a very important step in Eq. (1). It can be known from the definition of PDI that *M* represents the slope of soil line in Red-Nir space. For FY-3A/MERSI 250m resolution data, the bare soil points can be approximately acquired through the analysis of Red-Nir space. So as the slope of soil line can be estimated. In this study, *M* is calculated from Red-Nir space plotted from FY-3A/MERSI data dated on August 8, 2009, *M*=0.57. Therefore, the PDI formula can be expressed as follows,

$$\mathrm{PDI}=\frac{1}{\sqrt{0.57^2+1}}(R_{\mathrm{red}}+0.57R_{\mathrm{nir}}) \quad (2)$$

Drought guidelines based on PDI is another important step for evaluation of drought status. According to Qin *et al*. s (2008) study and the relationship between PDI and field soil water content measurements, the final PDI based drought guidelines are decided. Relative soil water content (RSWC) is the ratio of real soil water content to potential soil water content. Generally speaking, soil with RSWC above 75% is very wet and has ideal water condition for crop growth, and therefore defined as normal water condition and no drought happened. When RSWC varies between 45% and 75%, soil water is not sufficient for crop growth and is here termed as slight drought. When RSWC varies between 15% and 45%, drought status is further devel-

oped and moderate drought happen. Finally, when RSWC is below 15%, which is under the wilting coefficient, crop can not get any water from soil and severe drought happened. According to the relationship between PDI and the real RSWC, the following drought guidelines are determined (Table 1).

**Table 1 Relationship between PDI, relative soil water content and drought guidelines**

| Drought guidelines | Relative soil water content/% | PDI |
|---|---|---|
| Normal | >75 | <0.26 |
| Drought-slight | 45—75 | 0.26—0.33 |
| Drought-moderate | 16—45 | 0.33—0.40 |
| Drought-severe | <16 | >0.40 |

Drought status of the study area was evaluated on August 8, 13 and 20, 2009 using PDI based drought guidelines (Fig. 3—Fig. 5). According to the monitoring results derived from image of August 8, 2009, we can see that, large area of Chifeng and Tongliao was suffered from drought. Moderate drought was located in the middle and southwest of Tongliao and the middle and east of Chifeng. Obvious severe drought happened in the middle of Chifeng. It is reported from Inner Mongolia weather bureau that there was less than 10mm precipitation in the northwest of the study area on August 9, 2009. Compared to Fig. 3, up to August 13, 2009, area of slight drought and severe drought was decreased (Fig. 4) due to the precipitation on August 9, 2009. There was a obvious rainfall process in the north-middle of Tongliao and west-south of Chifeng during August 16—19, 2009, the precipitation in part was larger than 20mm, which is helpful for reduce water stress of the drought area. As shown in Fig.5, up to date August 20, 2009, area of slight drought and moderate drought was further decreased (Fig. 5) compared to August 13, 2009, drought status was observably eased. However, there was still large area of drought in the middle of Chifeng due to less precipitation in that area.

According meteorological information from Inner Mongolia weather bureau, in the beginning of August 2009, the precipitation was continuously less and the temperature was continuously higher, which is especially disadvantageous for crop growth. The precipitation is only 5mm in large part of Chifeng and part of Tongliao, which decreased 85% compared to the same period of the past years. Therefore, severe drought happened in that area. Soil water content report of the first 10 days of August 2009 from Inner Mongolia weather bureau also indicated favorable soil water content condition in north and part of middle of Tongliao and north of Chifeng. While in the middle and south of Tongliao and middle of Chifeng, soil water content condition reduced to a very low degree, indicating severe drought happened there. In the middle of August 2009, soil water content condition of the study area is better than the beginning of August 2009 due to the influence of rainfall process, especially in the north and south-west of Tongliao and north and south of Chifeng. While severe water stress is sustaining in the middle of Chifeng.

Compared Fig.3—Fig.5 to the history meteorological information, we can see that the PDI based drought monitoring results

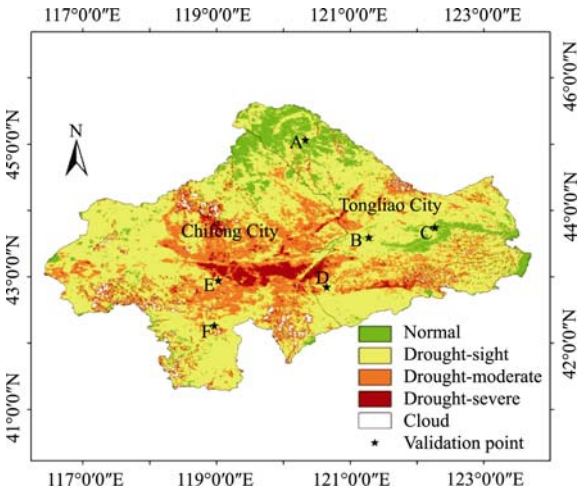


Fig. 3 Drought status of Tongliao and Chifeng (August 8, 2009)

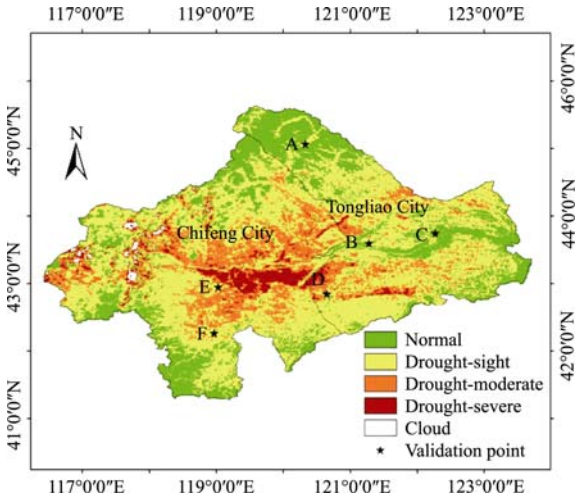


Fig. 4 Drought status of Tongliao and Chifeng (August 13, 2009)

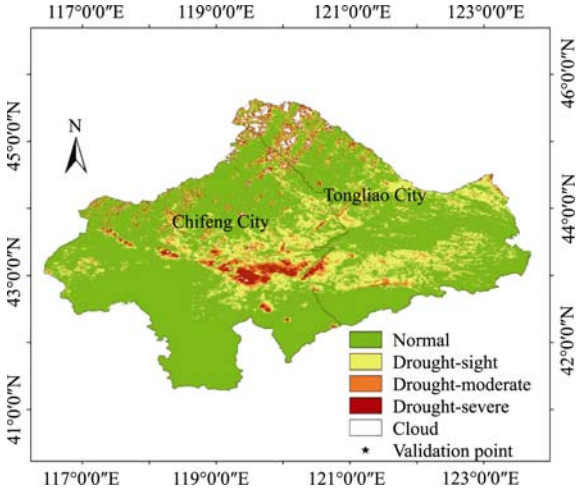


Fig. 5 Drought status of Tongliao and Chifeng (August 20, 2009)

are highly accordant with the real drought status and soil water condition. Our study demonstrates the feasibility of time series FY-3A/MERSI images and PDI drought index in displaying the spatial distribution and the development of drought.

## 5 VALIDATION

Since the PDI delivers information about the soil moisture status, relating PDI and real soil water content is the direct way for validation. In this study, scatter plot of PDI and field soil water content measurement is used for this purpose. There are six soil water content measurements on August 8 and 13, 2009, which are respectively point A (120.33°E,45.07°N), B (121.28°E, 43.59°N), C (122.27°E, 43.75°N), D (120.65°E,42.85°N), E (119.03°E, 42.95°N), F (118.97°E, 42.27°N) (Fig. 3—Fig. 4).

The validation results on August 8, 2009 are shown in Fig. 6—Fig. 7. It is shown from the results that there are significant negative correlations between the PDI and 10cm, 20cm depth soil water content, with the correlation coefficient $R^2$>0.65.

Relationship between PDI and 10cm, 20cm soil water content on August 13, 2009 were further plotted. Since only soil water content measurements on 8, 18, 28 are available for routine meteorological observation stations, filed soil water content on August 13, 2009 was approximately acquired by calculating the average of soil water content on August 8, 2009 and August 18, 2009. In this study, there is only small amount of rainfall (less than 10mm) in the north of the study area from August 8, 2009 to August 18, 2009. Therefore, taking the average soil water content of two adjacent times is feasible. The relationship between PDI and 10cm, 20cm soil water content on August 13, 2009 are shown in Fig.8—Fig.9. It is found that there is obvious negative correlation between PDI and 10cm soil water content measurements as shown in Fig.8 with $R^2$=0.41. Compared to 10cm soil water content, the correlation between PDI and 20cm soil water content measurements obviously increased ($R^2$=0.69) (Fig.9). As discussed above, in the process of calculating of soil water content on August 13, 2009, the average soil water content of two adjacent times is used. Therefore, error is inevitably introduced. This is the reason that the correlations between PDI and 10cm and 20cm soil water content on August 13, 2009 are lower than that the correlations on August 8, 2009.

Generally speaking, PDI has significant correlations with 10cm and 20cm depth soil water content (Fig.6—Fig.9). The correlation between PDI and 20cm depth soil water content is more significant than the correlation between PDI and 10cm depth soil water content. Although the reflectance of red and near infrared channels of satellite sensor is mainly from land surface, for 10cm depth soil water content, it is easily influenced by land surface wind speed and other meteorological conditions (Ghulam, 2006). Therefore, soil water content of 10cm depth can not fairly be related to the reflectance of land surface. Compared to 10cm depth soil water content, soil water content at 20cm depth is nearer the crop root, which is more sensible to crop water stress (Li *et al*., 1996). Therefore, the

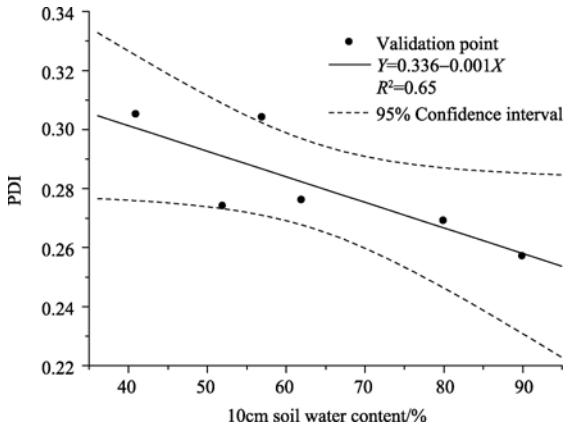


Fig. 6 Relationship between PDI and 10cm soil water content (August 8, 2009)

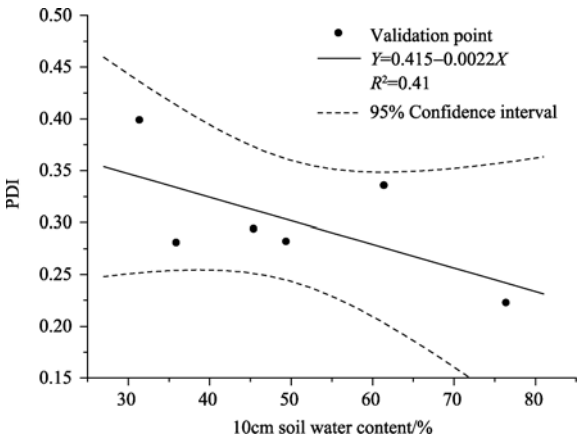


Fig. 8 Relationship between PDI and 10cm soil moisture (August 13, 2009)

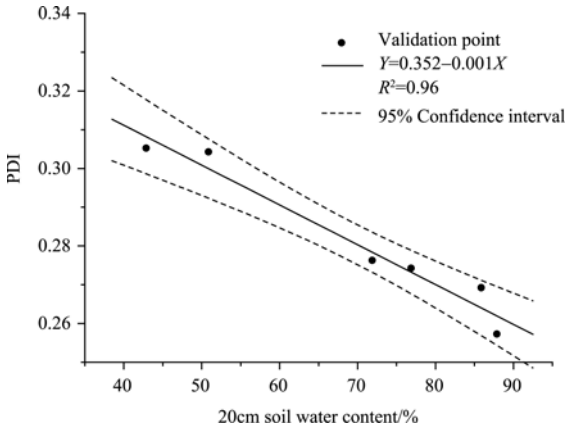


Fig. 7 Relationship between PDI and 20cm soil water content (August 8, 2009)

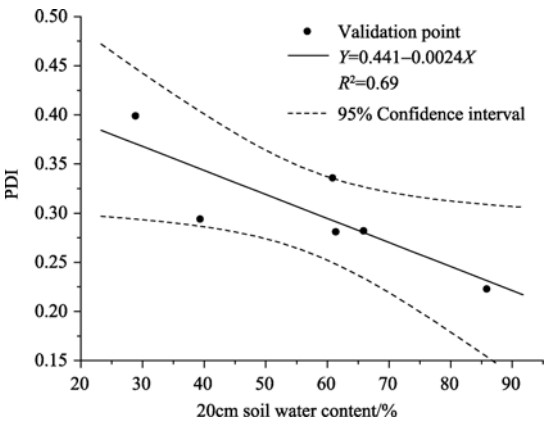


Fig. 9 Relationship between PDI and 20cm soil moisture (August 13, 2009)

relationship between PDI and 20cm depth soil water content is more stable. Li *et al*. (1996) compared the relationship between NDVI derived from NOAA/AVHRR and 10cm, 20cm depth soil water content. It is suggested that the correlation is obvious higher for 20cm depth soil water content and NDVI than 10cm depth soil water content and NDVI. Ghulam (2006) calculated PDI based on $ETM^+$ image and related PDI with field soil water content measurement at different depth. It is demonstrated that PDI is highly related to 10—20cm depth soil water content. Qin *et al*. (2008) validated the effective of PDI using MODIS 1km resolution images, and confirmed the stable relationship between PDI and 20cm depth soil water content. Compared to MODIS 1km image, FY-3A/MERSI has 250m spatial resolution, which reduces the noise of mixed-pixel and further improves the correlation between PDI and 20cm soil water content. The validation result of this study gave further support to above findings and shows great potential of FY-3A/MERSI images in drought monitoring applications.

## 6 CONCLUSION AND DISCUSSION

Medium Resolution Spectral Imager (MERSI) on board the new Generation Polar-Orbiting Meteorological Satellite of China (FY-3) are to provide global, quantitative, high spatial resolution remote sensing data under all weather conditions, which will greatly help drought monitoring research and application in China. In this study, FY-3A/MERSI data and PDI are used to monitor drought event happened in the summer of 2009 over the northeast of Inner Mongolia Autonomous Region, China. Results show that drought status derived from PDI is highly accordant with field drought observation. FY-3A/MERSI based PDI has significant correlation with 10cm and 20cm depth soil water content. Compared with 10cm depth soil water content, PDI has more stable relationship with 20cm depth soil water content. It is demonstrated that FY-3A/MERSI data has shown great potential in drought monitoring applications.

However, PDI is based on the concept of a fixed soil line in Red-Nir space. In reality, the shape of soil line is influenced by soil texture, soil water condition, fertilization and mix-pixel condition. The straight line property of soil line is only true in some spatial and temporal range. Therefore, *M* value in calculating PDI should be dynamic in large area with great land cover difference and long time span. Considering that the time range is very short and the study area only cover two cities in this study, *M* could be regarded as a fix value. This assumption could be one of the error sources in final drought monitoring result. Furthermore, remote sensing data used in this study has a spatial resolution of 250m, which can not directly match the field measurements of soil water content. Finally, drought guidelines based on PDI in this study is based on the analysis of the relationship between PDI and field soil water content measurements. It may be dynamic change due to atmosphere condition, the angle of remote sensor, land vegetation cover type and crop growth stage. The effect of PDI dynamic will be the main scope of our future work.

## REFERENCES


Ghulam A. 2006. Remote Monitoring of Farmland Drought based on n-Dimensional Spectral Feature Space. Peking University Ph.D. Thesis

Ghulam A, Qin Q and Zhan Z. 2007a. Designing of the perpendicular drought index. *Environmental Geology*, **52**(6): 1045—1052

Ghulam A, Qin Q, Teyip T and Li Z L. 2007b. Modified perpendicular drought index (MPDI): a real-time drought monitoring method. *ISPRS Journal of Photogrammetry and Remote Sensing*, **62**: 150—164

Ghulam A, Li Z L, Qin Q, Tong Q,Wang J, Alimujiang K and Lin Z. 2007c. A method for canopy water content estimation for highly vegetated surfaces–shortwave infrared perpendicular water stress index. *Science in China Series*. D, **50**(9), 1359—1368

Kogan F N. 1990. Remote sensing of weather impacts on vegetation in non-homogeneous areas. *International Journal of Remote Sensing*, **11**(8): 1405—1419

Kogan F N. 1995. Application of vegetation index and brightness temperature for drought detection. *Advances in Space Research*, **15**(11): 91—100

Li X C and Dong W M. 1996. Methods research on monitoring drought by using remote sensing and GIS. *Remote Sensing Technology and Application*, **11**(3): 7—15

Mcvicar T R and Jupp D L B. 1998. The current and potential operational uses of remote sensing to aid decisions on drought exceptional circumstances in Australia: a review. *Agricultural System*, **57**(3): 399—468

Njoku E G and Li L. 1999. Retrieval of land surface parameters using passive microwave measurements at 6—18 GHz. *IEEE Transactions on Geoscience and Remote Sensing*, **37**(1): 79—93

Price J C. 1985. On the analysis of thermal infrared imagery: the limited utility of apparent thermal inertia. *Remote Sensing of Environment*, **18**(1): 59—73

Qi S, Wang C, Niu Z and Liu Z. 2004. SVI and VCI based on NDVI time-series dataset used to monitor vegetation growth status and its response to climate variables. *Progress in Geography*, **23**(3): 91—99

Qin Q, Ghulam A, Zhu L, Wang L, Li J and Nan P. 2008. Evaluation of MODIS derived perpendicular drought index for estimation of surface dryness over northwestern China. *International Journal of Remote Sensing*, **29**(7): 1983—1995

Richardson A J and Wiegand C L. 1977. Distinguishing vegetation from soil background information. *Photogramm Eng Remote Sens*, **43**(12): 1541—1552

Sandholt I, Rasmussen K and Andersen J. 2002. A simple interpretation of the surface temperature/vegetation index space for assessment of surface moisture status. *Remote Sensing of Environment*, **79**(2—3): 213—224

Schmugge T, O'Neill P E and Wang J R. Passive microwave soil moisture research. *IEEE Transactions on Geoscience and Remote Sensing*, 1986, **24**(1): 12—22

She W M and Ye C H. 2006. Review on soil moisture and drought remote sensing monitoring based MODIS satellite data. *Meteorology Journal of Henan*, (1): 44—46

Song X N and Zhao Y S. 2004. Study on vegetation-temperature-water synthesis index using MODIS satellite data. *Geography and Geo-Information Science*, **20**(2): 13—17

Tan D B, Liu L M, Yan J J and Hu Y. 2004. Research on drought monitoring model based on MODIS data. *Journal of Yangtze River Scientific Research Institute*, **21**(3): 11—15

Xiao Q, Chen W, Sheng Y and Li J. 1994. A study on soil moisture monitoring using NOAA satellite. *Quarterly Journal of Applied Meteorology*, **5**(3): 312—318

Yang J ,Dong C H , Lu N M ,Yang Z D , Shi J M, Zhang P ,Liu Y J and Cai B. 2009. FY-3A: the new generation polar-orbiting meteorological satellite of China. *Acta Meteorologica Sinica*, **67**(4): 501—509

Zhan Z M, Qin Q M, Ghulam A and Wang D D. 2007. Nir–red spectral space based new method for soil moisture monitoring. *Science in China Ser. D*, **50**(2): 283—289

Zhang W Z, Yao S R, Zhao C L and Wang Y X. 2006. New method for drought monitoring and pre-warning with EOS/MODIS. *Meteorogical Science and Technology*, **34**(4): 501—504

# FY-3A/MERSI 数据在中国北方干旱监测中的应用

朱 琳, 刘 健, 张晔萍, 王 萌

国家卫星气象中心 北京 100081

摘 要: 中国新一代极轨气象卫星风云 3 号 A 星(简称 FY-3A)上搭载的中分辨率光谱成像仪(MERSI)具有 5 个 250m 分辨率通道, 进一步加强了对地表精细地物的观测能力, 为大面积干旱监测提供了新的遥感数据源。利用 FY-3A/MERSI 传感器 250m 分辨率数据和垂直干旱指数(perpendicular drought index,PDI)对 2009 年夏季内蒙古自治区中东部干旱进行了监测。结合气象部门的降水、温度和气象干旱资料对比分析表明, 基于 250m 分辨率的时序 FY-3A/MERSI 卫星资料反演的 PDI 干旱指数能够客观地反映研究区旱情的空间分布和动态发展过程。利用实地观测的土壤水分数据验证了 PDI 指数和土壤水分之间的关系。从验证结果看: PDI 指数和对应实地观测的 10cm、20cm 土壤持水百分含量之间有较好的负相关关系, 其中 PDI 和 20cm 深度处的土壤持水百分含量之间的相关关系更为稳定, $R^2$ 达到 0.69 以上。该研究表明利用中国新型、自主的 FY-3A 卫星资料进行干旱监测业务是可行的。

关键词: FY-3A/MERSI 遥感数据, 干旱监测, 垂直干旱指数, 土壤水分

中图分类号: TP79 文献标志码: A

**引用格式**: 朱 琳, 刘 健, 张晔萍, 王 萌. 2010. FY-3A/MERSI 数据在中国北方干旱监测中的应用. 遥感学报, **14**(5): 1004—1016

Zhu L, Liu J, Zhang Y P and Wang M. 2010. Application of FY-3A/MERSI satellite data to drought monitoring in north China. *Journal of Remote Sensing*. **14**(5): 1004—1016

## 1 引 言

近年来, 随着全球气候变化、地区经济快速发展和人口增长的共同影响, 大范围干旱发生频繁, 对国民经济和农业发展造成了严重影响。如 2008 年冬季到 2009 年春季发生在全国冬麦区大范围的干旱, 持续时间长、受旱范围广、受旱程度重是历史少见的。2009 年夏秋, 在中国内蒙古自治区中东部、东北地区西部和湖南、贵州、广西等省降水持续偏少, 出现了大面积的干旱, 对这些地区正值生长期的作物产生严重影响。因此研发一套有效、动态、切实可行的干旱监测方法和业务监测流程, 不仅可为防旱抗旱、科学灌溉、提高农作物产量提供决策依据, 同时也对深入探索气候变化的成因及发展趋势具有非常重要的意义。

遥感具有高度的空间概括能力和地物分辨能力, 与地面观测相比, 利用遥感方法进行大范围旱情动态监测具有一定的优势。20 世纪 70 年代以来, 研究人员采用可见光-近红外(Kogan, 1990; 肖乾广等, 1994; 齐述华, 2004; Zhan 等, 2007; Ghulam 等, 2007a, 2007b, 2007c)、热红外(Price, 1985; Kogan, 1995; Mcvicar & Jupp, 1998; Sandholt 等, 2002)或微波遥感(Schmugge 等, 1986; Njoku & Li, 1999)影像获取农田水分信息, 构造了大量的遥感干旱监测模型, 为大面积干旱监测提供有效的方法。目前国内遥感干旱监测以 NOAA/AVHRR、Landsat/TM、TERRA/AQUA 星载的 MODIS 等传感器获得的影像为主要数据源(佘万明 & 叶彩华, 2006)。特别是在 TERRA 和 AQUA 卫星上搭载的 MODIS 传感器以其适中的空间分辨率、高光谱分辨率和时间分辨率等优点, 不仅广泛在已有的干旱监测模型上加以应用和验证, 而且用来构造新的干旱监测指数。谭德宝等(2004)利用 MODIS 数据提出了一个综合植被指数、昼夜温差、降水距平、前期干旱情况等的综合干旱监测模型。宋小宁等(2004) 利用 MODIS 可见光、近红外和热红外波段构造了反映植被-温度-水分

收稿日期: 2009-10-29; 修订日期: 2010-04-18

基金项目: 国家自然科学基金(编号: 40771148)和气象行业专项项目(编号: GYHY200806022)。

第一作者简介: 朱琳(1978— )女, 博士, 2009 年毕业于北京大学遥感与地理信息系统研究所。目前主要从事遥感土壤水分和植被监测理论基础及应用研究。E-mail: zhulin@cma.gov.cn。

状况的综合指数。张蓓等(2004)利用 MODIS 数据和 GVMI(global vegetation moisture index)指数模型反演出植被水分含量信息, 分析了植被水分含量与区域旱情状况之间的关联性。张文宗等(2006)利用 MODIS 数据提出了能量指数模式, 并用来改进云对常规热惯量法的干扰。Qin 等(2008)利用 MODIS 数据反演了垂直干旱指数(perpendicular drought index, PDI), 并将其应用到中国北方干旱区的干旱监测研究中, 结合当地的土壤、水文等特征参数将 PDI 划分为不同的干旱等级。研究表明, PDI 仅由红光、近红外两个波段计算而得, 操作简单, 易于获取。此外, 由 PDI 干旱指数获得的干旱分布状况和实际的干旱情况相一致, 这为利用 MODIS 数据大面积监测干旱提供了有效的方法。

随着中国新一代极轨气象卫星风云三号(FY-3)气象卫星的研制和开发, 大大增强了中国地表生态过程监测的能力, 为大面积干旱监测提供了新的遥感数据源。FY-3 系列的第 1 颗星——风云 3 号 A 星(FY-3A)已于 2008-05-27 11:02:33 在山西太原卫星发射中心成功发射(杨军等, 2009)。FY-3A 上搭载了 11 个传感器, 其中的中分辨率光谱成像仪(MERSI)具有 5 个 250m 分辨率的通道和 15 个 1km 分辨率的通道, 同时具有了多光谱和高分辨率的特点。与地球观测系统 EOS/TERRA/AQUA 星载的 MODIS 传感器相比, FY-3A/MERSI 传感器加强了对地表精细地物的观测能力, 将 250m 分辨率通道数从 MODIS 的 2 个增加到 5 个, 特别是包含 1 个 10.5—12.5μm 的热红外通道, 实现了利用中国极轨卫星数据对气象灾害和环境灾害的中分辨率遥感监测。因此, 中国的 FY-3A/MERSI 遥感卫星具有比 MODIS 更为优越的应用潜力。进一步研究利用 FY-3A/MERSI 数据对中国大面积干旱连续监测, 对提升中国卫星遥感自主应用能力、在业务系统中减少对国外遥感数据的依赖、确保中国干旱监测的及时性和准确性具有十分重要的意义。

本文利用 FY-3A/MERSI 传感器数据, 以 2009 年夏季发生在中国内蒙古自治区中东部、东北地区西部干旱事件为例, 尝试对该地区的干旱情况进行遥感监测和分析, 为中国自主新型遥感数据的应用和相关部门减灾防灾提供借鉴和决策支持。

## 2　研究区与数据

### 2.1　研究区概况

本文以内蒙古自治区东部的通辽市和赤峰市为研究区域。研究区地理坐标为 116°21′—123°43′E, 41°17′—45°59′N, 属于典型的半干旱大陆性季风气候, 冬季漫长寒冷, 夏季干旱多风, 年平均气温 0℃—7℃, 年平均降水量 350—500mm。干旱是研究区内气候的一大特点, 几乎历年不同季节均有不同程度的发生。

### 2.2　数据来源与预处理

FY-3A/MERSI 具有 20 个通道, 其中第 3 通道(红光:中心波长 0.650μm, 光谱带宽: 0.05μm)和第 4 通道(近红外:中心波长 0.865μm,光谱带宽: 0.05μm)具有 250m 地面分辨率, 并处于对植被光谱特征比较敏感的范围内。本研究采用的 FY-3A/MERSI 原始数据来源于中国气象局国家卫星气象中心, 数据采用 HDF5 文件格式。通过国家卫星气象中心自主开发的图像处理软件, 实现了 MERSI 数据的多通道定标、地理定位和拼接等预处理, 生成地面分辨率为 250m 的 ENVI 可以直接读取的 LDF 格式的数据集。最后利用 ENVI 进行投影转换和研究区的裁减。

为了便于地面验证分析, 收集了 2009 年 8 月 8 日、18 日 6 个标准气象站的浅层土壤水分数据, 包括地表 10cm、20cm 深处土壤持水百分率。土壤水分数据按国家气象局编订的农业气象观测规范测定。此外还收集了研究时段内蒙古气象局发布的旬干旱监测报告、农业气象旬报、逐日降雨量和气温等实况资料。

## 3　垂直干旱指数模型

早在 20 世纪 70 年代, 就有研究者开始对红光-近红外二维光谱特征空间中植被变化规律进行研究。由于植被对红光有强烈的吸收, 对近红外有强烈反射,通过红光和近红外数学变换计算植被指数, 达到植被长势监测的目的。Richardson 和 Wiegand(1977)根据植被在红光-近红外光谱特征空间的分布规律, 用在红光-近红外光谱特征空间任一点到土壤线的垂直距离描述植被覆盖情况, 提出了垂直植被指数(PVI)。同时, 由于水体对红光和近红外波段吸收很强, 土壤含水量是影响土壤在红光和近红外反射率的主要因素。Jackson(1983)描述了水分在红光-近红外光谱特征空间的分布特征。前者从理论基础到数学模型已经相当成熟, 在植被、作物长势监测和遥感估产等方面得到广泛使用。

詹志明等(2006)、阿布都瓦斯提• 吾拉木 (2006)的进一步研究表明, $ETM^{+}$图像波段 4(红光:0.630—

0.690μm)和波段 5(近红外: 0.775—0.90μm)组成的二维散点图呈典型的三角形, 三角形的下边线周围的点通常对应图像中的裸露土壤点。将这些点进行线性回归, 得到一条反映土壤在近红外和红光波段反射率关系的直线, 即通常所说的土壤线(Richardson 和 Wiegand, 1977)。阿布都瓦斯提• 吾拉木 (2006)将这种三角形关系抽象出来, 得到图 1: *AD* 线代表地表植被生长状况从全覆盖(*A* 点)到部分覆盖(*E* 点)到无植被覆盖(*D* 点)。在这一“ 三角形 ”特征空间中, 不仅地表植被覆盖情况而且地表水分状况和干旱程度能够被定量的表现出来。水体分布在土壤线靠近 *B* 点一侧, 湿土分布在土壤线的中部而干土分布在土壤线靠近 *C* 点一侧。*BC* 一线的变化代表土壤水分状况的变化: 分别为湿润(*B*)、半湿润(*D*)到极端干旱区(*C*)。因此, *B*—*D*—*C* 一线说明了干旱程度加重的方向。

基于上述变化规律, 阿布都瓦斯提• 吾拉木 (2006) 利用 ETM$^+$图像波段 4(红光:0.630—0.690μm)和波段 5(近红外: 0.775—0.90μm)组成的二维散点图构造了垂直干旱监测指数 (perpendicular drought index, PDI)(图 2)。在红光和近红外光谱组成的二维光谱特征空间中(图 2), 首先过原点(0, 0)作一条垂直于土壤线 *BC* 的直线 *L*。图像中任一点的 PDI 值是从该点出发, 平行于土壤线(*BC* 线)且和直线 *L* 垂直相交的一条线段的长度。如: *E* 点的 PDI 值对应从 *E* 点出发, 并垂直于直线 *L* 的线段 *EF* 的长度。PDI 指数描述了在红光-近红外光谱特征空间中土壤水分的分布规律: PDI 值越高的点对应着土壤含水量低的区域; 反之, PDI 值越低的点对应着土壤含水量越高的区域。

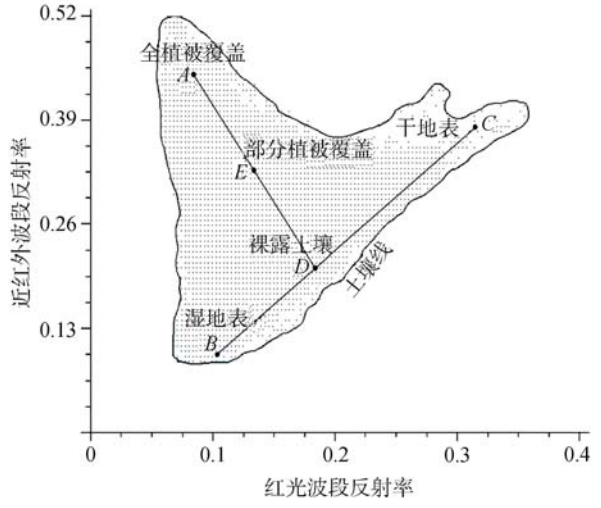


图 1 利用 ETM$^+$图像构建的红光-近红外光谱特征空间
(引自: 阿布都瓦斯提・吾拉木(2006))

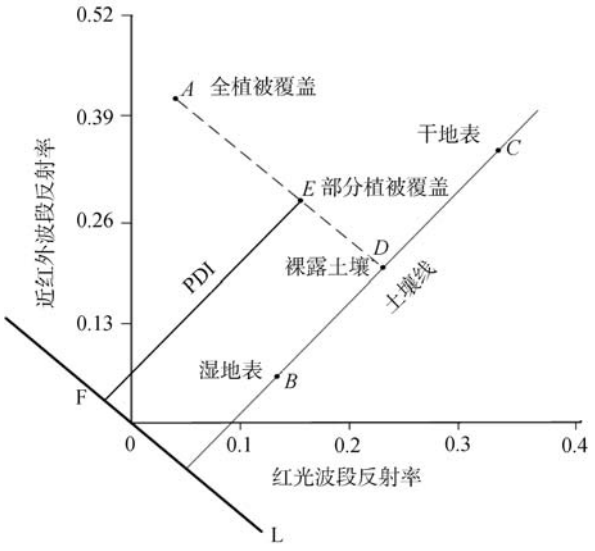


图 2 PDI 构建
(引自: 阿布都瓦斯提・吾拉木 (2006))

PDI 的数学表达式如下(阿布都瓦斯提• 吾拉木, 2006):

$$\mathrm{PDI}=\frac{1}{\sqrt{M^2+1}}(R_{\mathrm{red}}+MR_{\mathrm{nir}}) \tag{1}$$

式中, $R_{\mathrm{red}}$ 和 $R_{\mathrm{nir}}$ 分别代表红光和近红外波段遥感数据, *M* 代表根据红光-近红外二维光谱特征空间中对土壤点进行线性回归得到的土壤线的斜率。PDI 的值在 0—1 之间, PDI 越大表示干旱程度越严重; 越小表示水分胁迫越少。PDI 简单实用, 易于操作和获取, 在实际应用中, 仅仅从红光-近红外的光谱特征空间就可以有效地对地表干旱进行实时监测。

## 4 干旱监测图的制作和结果分析

为了验证基于 FY-3A/MERSI 数据的 PDI 干旱监测模型在中国北方干旱监测中的应用效果, 选取研究区 2009-08-08、2009-08-13 和 2009-08-20 三个时次的 FY-3A/MERSI 数据。遥感数据时间上选择的依据主要考虑以下两点因素: (1) 在所选的 3 个时间点, 研究区晴朗干燥少云, 使得 PDI 反演时受云和大气状况的影响最小, 故在数据预处理时略去了大气校正和云检测的步骤; (2) 8 月份以来, 研究区降雨量少, 地表温度持续偏高, 因此所选的第一个时间点(2009-08-08)能够反映该地区干旱的严重程度。在 2009 年 8 月 8—13 日和 13—20 日两个时段内, 研究区有不同程度的降雨。反演以上时间的 PDI 干旱指数便于对比 FY-3A/MERSI 时间序列数据对干旱程度变化的敏感性。

FY-3A/MERSI 第 3 通道(红光)和第 4 通道(近红外)的反射率影像经过几何校正等预处理后, 通过公式(1)计算 PDI 指数。公式(1)中 $M$ 值的确定是计算 PDI 的关键步骤之一。由 PDI 的定义可知: $M$ 值代表根据红光-近红外光谱特征空间中土壤点线性回归得到的土壤线的斜率。对于 FY-3A/MERSI 第 3 和第 4 通道, 地面分辨率是 250m, 通过分析研究区域的红光-近红外反射率光谱二维散点图中裸地光谱反射率信息, 可找出近似纯裸土像元, 据此进行线性回归, 提取土壤线。根据研究区 2009-08-08 FY-3A/MERSI 遥感影像红光-近红外反射率光谱二维散点图提取土壤线, 确定 $M$=0.57。从而, PDI 的计算公式可表示如下:

$$\mathrm{PDI}=\frac{1}{\sqrt{0.57^2+1}}(R_{\mathrm{red}}+0.57R_{\mathrm{nir}}) \qquad (2)$$

计算 PDI 指数后,建立 PDI 和干旱程度的分级标准间的对应关系, 是确定干旱程度的另一个重要步骤。通过分析 PDI 和实际的土壤相对含水量间的关系, 参考 Qin 等(2008)对 PDI 干旱指数分级的研究, 建立最终的分级标准。土壤相对含水量是实际的土壤含水量和土壤最大持水量的比值。一般来说, 土壤相对含水量大于 75%时, 土壤中的水分最适合作物的生长, 该地区比较湿润, 可以界定为不发生干旱的临界范围; 当土壤相对含水量在 45%—75%时, 水分基本上能够维持作物正常生长, 但不充足, 发生轻度干旱; 当土壤相对含水量在 16%—45%时, 干旱情况进一步加重, 可界定为中度干旱; 当土壤相对含水量小于 16%时, 对应地表的含水量已经小于作物的调萎系数, 对作物的生长产生严重影响, 发生重度干旱。表 1 给出了 PDI、土壤相对含水量和干旱等级之间的对应关系。

**表 1　PDI、土壤相对含水量和干旱等级间的对应关系**

| 干旱等级 | 土壤相对含水量/% | PDI 干旱指数 |
|---|---|---|
| 正常 | >75 | <0.26 |
| 轻度干旱 | 45—75 | 0.26—0.33 |
| 中度干旱 | 16—45 | 0.33—0.40 |
| 重度干旱 | <16 | >0.40 |

利用上述干旱分级标准, 对 2009 年 8 月份内蒙古自治区东部的通辽市和赤峰市开展了动态卫星遥感干旱监测, 监测结果如图 3—图 5。图 3 反映出 2009 年 8 月上旬, 通辽市和赤峰市出现较大范围的旱区, 中等以上的干旱主要分布在通辽市中部和西南部、以及赤峰市的中东部, 特别是在赤峰市中部重旱面积较大。2009-08-09 研究区西北部有 10mm 以内的降水。据 2009-08-13 的遥感干旱监测图显示(图 4): 与 2009-08-08 的遥感监测图相比, 8 月中旬前期, 通辽地区北部和赤峰大部受前期弱降水的影响, 轻旱和重旱范围有略微减少, 但大部分地区的旱情仍在持续。2009 年 8 月 16—19 日内蒙古自治区自西向东出现 2009 年入汛以来范围较大的、明显降水天气过程, 此次降水主要集中在通辽北部中部以及赤峰市西部和南部。其中赤峰市、通辽市局部累积降雨量在 20mm 以上, 对旱情的缓解有明显的作用。由图 5 可见, 与 8 月中旬前期相比, 研究区干旱得到一定程度的缓解, 表现在轻旱和中旱范围有所减少, 但由于赤峰市中部重旱区域降水量较小, 干旱情势仍然没有解除。

据内蒙古自治区气象部门降水和温度资料显示, 2009 年 8 月上旬, 内蒙古自治区中东部气温较常年偏高, 降水偏少, 对牧草和农作物的生长发育有较大影响。赤峰市大部、通辽市局部平均降水量 5mm,

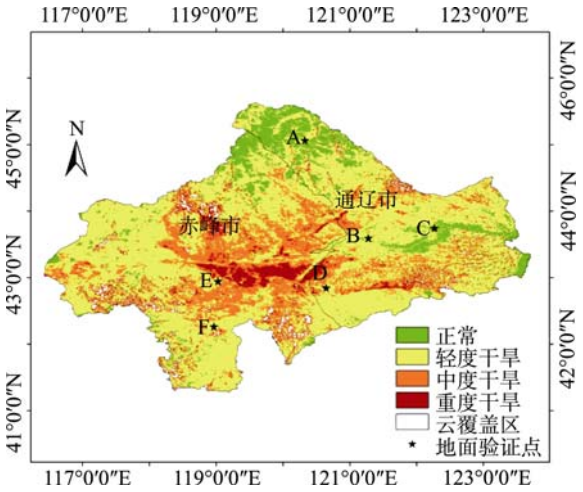


图 3　通辽市和赤峰市遥感干旱监测图(2009-08-08)

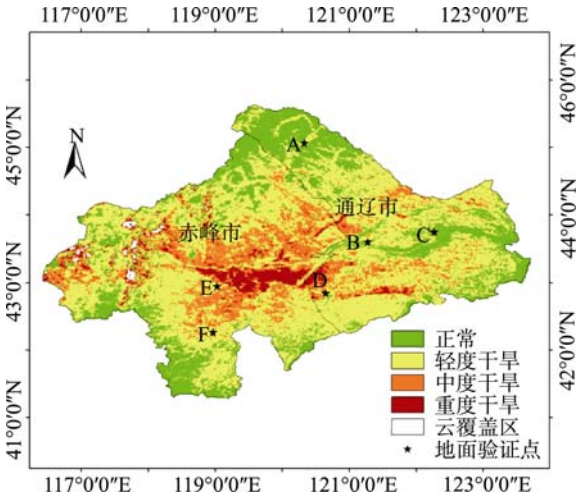


图 4　通辽市和赤峰市遥感干旱监测图(2009-08-13)

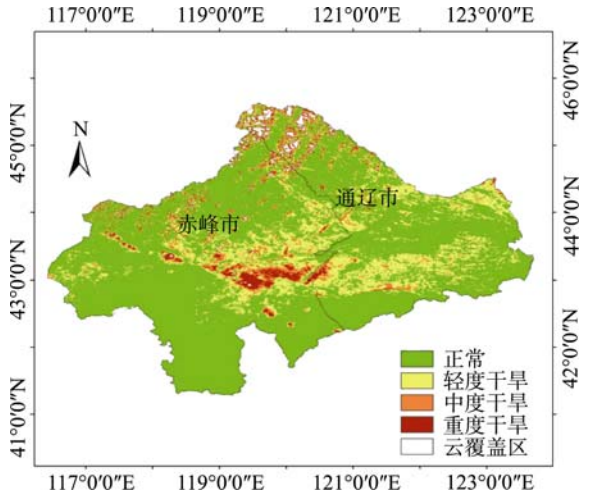


图 5 通辽市和赤峰市遥感干旱监测图(2009-08-20)

比历年同期减少 85%, 普遍发生严重夏旱。内蒙古自治区气象局发布的 2009 年 8 月上旬土壤墒情资料显示, 在通辽市北部和中部局部、赤峰市北部土壤墒情较好, 而在通辽市中部和南部、赤峰市中部土壤墒情降低到 3 类以下, 说明该地区受到干旱的威胁。在 2009 年 8 月中旬, 受降水的影响, 研究区土壤墒情均好于 8 月上旬, 一类及二类的土壤墒情主要分布在通辽北部和西南部、赤峰北部和南部, 赤峰中部的重旱区域土壤墒情仍然较差, 普遍在三类及以下。

对比气象部门的历史资料和图 3—图 5 可见, 遥感干旱监测结果和实际干旱和土壤墒情的分布比较吻合。利用时序的 FY-3A/MERSI 遥感影像和 PDI 干旱指数, 不仅能够给出研究区干旱空间分布, 还能够较好地反映干旱的动态变化。

## 5 干旱监测结果的验证

干旱和土壤水分含量密切相关。建立 PDI 干旱指数和实地测量的土壤水分含量之间的关系是验证干旱监测结果最直接的方法。利用散点图来考察 PDI 值和地面观测土壤水分值的相关性。考察研究区实际的土壤水分监测资料有 6 个常规农业气象观测点对应有土壤水分监测结果, 它们分别是 *A*(120.33°E, 45.07°N) 、 *B*(121.28'E, 43.59°N) 、 *C*(122.27°E, 43.75°N) 、 *D*(120.65°E, 42.85°N) 、 *E*(119.03°E, 42.95°N)、*F*(118.97°E, 42.27°N) (图 3)。

试验结果如图 6—图 9。图 6、图 7 分别为 2009-08-08 PDI 干旱指数和对应测量的 10cm 深度处和 20cm 深度处的土壤持水百分含量的散点图和线性关系。可见, PDI 指数和对应的 10cm、20cm 土壤持水百分含量之间有较好的负相关关系, $R^2$ 达到 0.65 以上。

进一步考察了 2009-08-13 的 PDI 和地面土壤水分观测资料之间的关系。由于常规的地面土壤水分

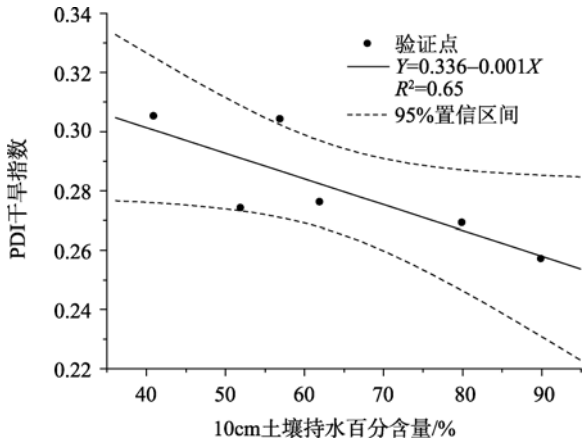


图 6 PDI 和 10cm 土壤持水百分含量的关系(2009-08-08)

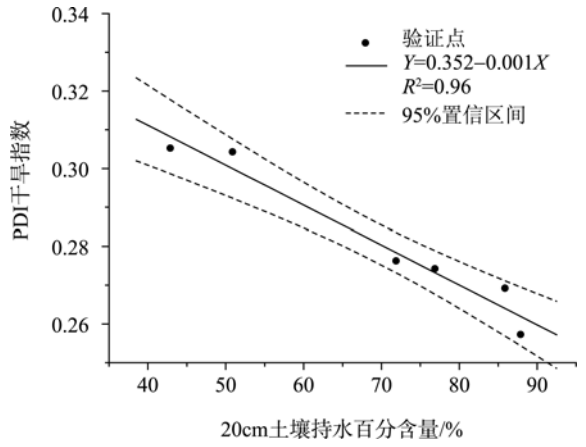


图 7 PDI 和 20cm 土壤持水百分含量的关系(2009-08-08)

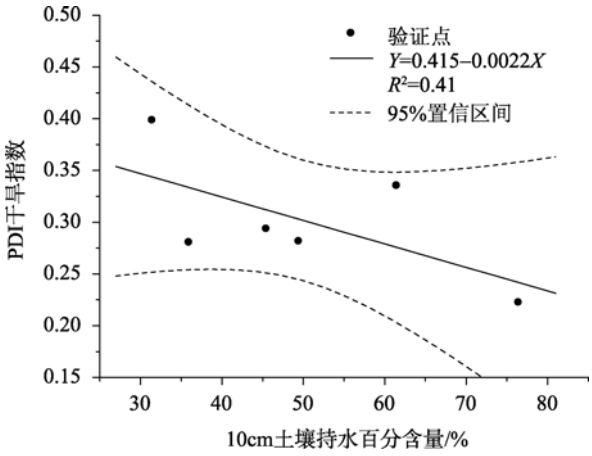


图 8 PDI 和 10cm 土壤持水百分含量的关系(2009-08-13)

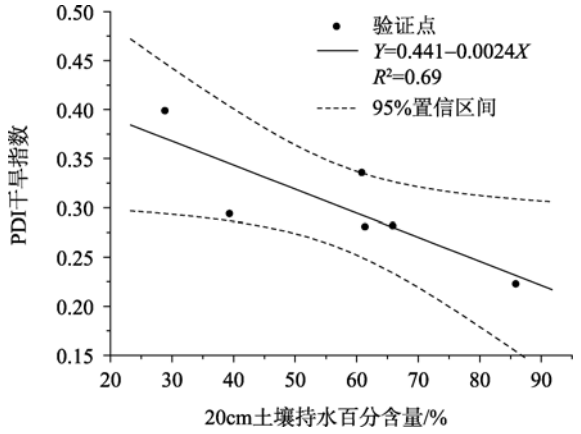


图 9　PDI 和 20cm 土壤持水百分含量的关系(2009-08-13)

观测时间是每月的 8 日、18 日和 28 日，对于 2009-08-13 的监测结果，作者采取了 2009-08-08 和 2009-08-18 的土壤持水百分含量的平均值作为 2009-08-13 的近似土壤持水百分含量。对比研究区 2009 年 8 月 08—18 日的每日降水量实况资料，发现在这个时段只有在 9 日、16 日、18 日在研究区北部有降水，且小于 10mm。由于降水量较少，总体上对这 6 个点的土壤水分的线性变化影响不大。

图 8 为 2009-08-13 PDI 干旱指数和对应的 10cm 深度处的土壤持水百分含量的散点图和线性关系。由图 8 可见，PDI 和 10cm 深度处土壤持水百分含量之间呈较好的负相关关系，$R^2$ 达到 0.41。对比 2009-08-13 PDI 干旱指数和对应的 20cm 深度处的土壤持水百分含量的散点图(图 9)发现，两者之间的负相关关系进一步增强，$R^2$ 达到 0.69。对本研究而言，采用 8 月 8 日和 8 月 18 日两个时间点的土壤水分平均值代替 8 月 13 日的土壤水分值，会带来一定的误差。8 月 13 日 PDI 和实测土壤水分之间的相关系数较 8 月 8 日有所降低。

比较图 6—图 9 的验证结果可见，总体上 PDI 指数和对应实地观测的 10cm、20cm 土壤持水百分含量之间有较好的负相关关系，20cm 土壤水分与 PDI 的相关关系比 10cm 土壤水分与 PDI 的相关关系更高。尽管可见光、近红外遥感测定的是地表“皮肤”的反射特性，对于 10cm 深度处土壤水分而言，受到地表风速和气象条件的影响较大(阿布都瓦斯提• 吾拉木，2006)，并不能完全反映地表反射率特性。同时，与 10cm 深处土壤水分相比，20cm 深处的土壤水分更接近作物根部，对作物的生长影响更大，因而更能反映作物的受旱情况(李杏朝 & 董文敏，1996)。因此， PDI 和 20cm 深度处的土壤水分含量之间的相关关系更为稳定。李杏朝和董文敏(1996)研究表明，20cm 深处的土壤水分与 NOAA/AVHRR 卫星资料计算的归一化植被指数(NDVI)的相关关系较 10cm 深处的土壤水分与 NDVI 的相关关系更好。阿布都瓦斯提• 吾拉木(2006)利用 $ETM^+$计算 PDI 干旱指数，并和不同深度处实测的土壤水分含量计算的干旱指数相比较，研究结果表明 PDI 和 10—20cm 范围的土壤水分具有较高的相关性。Qin 等(2008)利用 MODIS 1km 分辨率的数据在宁夏回族自治区对 PDI 的干旱监测效果进行了验证，证明 PDI 和 20cm 深度处土壤水分之间有稳定的相关关系，$R^2$ 达到 0.487。本文的研究结果进一步支持了以上论证。由于本文使用 FY-3A/MERSI 传感器 250m 分辨率的数据，与 MODIS 1km 的数据相比，减少了遥感混合像元的干扰，使得 PDI 和 20cm 深处的土壤水分之间的相关性显著提高。

综上所述，利用中国新型、自主的 FY-3A 卫星资料进行干旱监测业务是可行的。

## 6　结论与讨论

中国自主研发的新一代极轨气象卫星 FY-3A/MERSI 数据对干旱灾害监测具有全球、全天候、定量、地面分辨率高等优点，为大面积干旱监测提供了新的遥感数据源。本文采用 FY-3A/MERSI 数据和 PDI 干旱指数对中国北方典型的干旱半干旱区域进行了干旱监测试验。从卫星遥感监测结果和实地土壤水分数据和旱情监测资料对比来看，PDI 干旱指数能够较好地反映研究区干旱的发展和动态变化，并和实地观测的 10cm、20cm 土壤持水百分含量之间有较好的负相关关系。可见 FY-3A/MERSI 遥感数据在实际干旱监测业务工作中具有较大的应用潜力。

在本文中，PDI 的数学表达式是基于一条固定土壤线来确定的。由于土壤质地、水分含量、施肥状况、混合像元等因素的影响，红光-近红外二维光谱特征空间的土壤线的直线特征仅在一定空间和时间范围内存在，并非一条绝对意义上固定的直线。因此，PDI 中的 $M$ 值对于地表状况差异较大的区域和不同时间尺度是动态变化的。在本文中由于时间跨度较短、研究区仅覆盖内蒙古通辽和赤峰两市，$M$ 值设定为一固定的值，并认为 $M$ 值不随时间和空间而变化，这可能是引起最终干旱监测误差的原因之一。此外，由于所用的遥感数据的空间分辨率是 250m，直接和地面点的数据进行验证会存在尺度变化和混合像元的偏差。本文所建立的干旱分级指标是在对研究区实地的土壤水分和 PDI 的关系进行了

分析的基础上建立的。实际的 PDI 还受大气状况、传感器角度以及地表植被类型和生长发育阶段等多种因素的影响，在实际的业务中应注意 PDI 干旱分级标准的动态性。

## REFERENCES


Ghulam A. 2006. Remote Monitoring of Farmland Drought based on n-Dimensional Spectral Feature Space. Peking University Ph.D.Thesis

Ghulam A, Qin Q and Zhan Z. 2007a. Designing of the perpendicular drought index. *Environmental Geology*, **52**(6): 1045—1052

Ghulam A, Qin Q, Teyip T and Li Z L. 2007b. Modified perpendicular drought index (MPDI): a real-time drought monitoring method. *ISPRS Journal of Photogrammetry and Remote Sensing*, **62**: 150—164

Ghulam A, Li Z L, Qin Q, Tong Q,Wang J, Alimujiang K and Lin Z. 2007c. A method for canopy water content estimation for highly vegetated surfaces–shortwave infrared perpendicular water stress index. *Science in China Series*. D, **50**(9), 1359—1368

Kogan F N. 1990. Remote sensing of weather impacts on vegetation in non-homogeneous areas. *International Journal of Remote Sensing*, **11**(8): 1405—1419

Kogan F N. 1995. Application of vegetation index and brightness temperature for drought detection. *Advances in Space Research*, **15**(11): 91—100

Li X C and Dong W M. 1996. Methods research on monitoring drought by using remote sensing and GIS. *Remote Sensing Technology and Application*, **11**(3): 7—15

Mcvicar T R and Jupp D L B. 1998. The current and potential operational uses of remote sensing to aid decisions on drought exceptional circumstances in Australia: a review. *Agricultural System*, **57**(3): 399—468

Njoku E G and Li L. 1999. Retrieval of land surface parameters using passive microwave measurements at 6—18 GHz. *IEEE Transactions on Geoscience and Remote Sensing*, **37**(1): 79—93

Price J C. 1985. On the analysis of thermal infrared imagery: the limited utility of apparent thermal inertia. *Remote Sensing of Environment*, **18**(1): 59—73

Qi S H, Wang C Y, Niu Z and Liu Z Z. 2004. SVI and VCI based on NDVI time-series dataset used to monitor vegetation growth status and its response to climate variables. *Progress in Geography*, **23**(3): 91—99

Qin Q, Ghulam A, Zhu L, Wang L, Li J and Nan P. 2008. Evaluation of MODIS derived perpendicular drought index for estimation of surface dryness over northwestern China. *International Journal of Remote Sensing*, **29**(7): 1983—1995

Richardson A J and Wiegand C L. 1977. Distinguishing vegetation from soil background information. *Photogramm Eng Remote Sens*, **43**(12): 1541—1552

Sandholt I, Rasmussen K and Andersen J. 2002. A simple interpretation of the surface temperature/vegetation index space for assessment of surface moisture status. *Remote Sensing of Environment*, **79**(2—3): 213—224

Schmugge T, O'Neill P E and Wang J R. Passive microwave soil moisture research. *IEEE Transactions on Geoscience and Remote Sensing*, 1986, **24**(1): 12—22

She W M and Ye C H. 2006. Review on soil moisture and drought remote sensing monitoring based MODIS satellite data. *Meteorology Journal of Henan*, (1): 44—46

Song X N and Zhao Y S. 2004. Study on vegetation-temperature-water synthesis index using MODIS satellite data. *Geography and Geo-Information Science*, **20**(2): 13—17

Tan D B, Liu L M, Yan J J and Hu Y. 2004. Research on drought monitoring model based on MODIS data. *Journal of Yangtze River Scientific Research Institute*, **21**(3): 11—15

Xiao Q G, Chen W Y, Sheng Y W and Li J. 1994. A study on soil moisture monitoring using NOAA satellite. *Quarterly Journal of Applied Meteorology*, **5**(3): 312—318

Yang J ,Dong C H , Lu N M ,Yang Z D , Shi J M, Zhang P ,Liu Y J and Cai B. 2009. FY-3A: the new generation polar-orbiting meteorological satellite of China. *Acta Meteorologica Sinica*, **67**(4): 501—509

Zhan Z M, Qin Q M, Ghulam A and Wang D D. 2007. Nir–red spectral space based new method for soil moisture monitoring. *Science in China Ser. D*, **50**(2): 283—289

Zhang W Z, Yao S R, Zhao C L and Wang Y X. 2006. New method for drought monitoring and pre-warning with EOS/MODIS. *Meteorogical Science and Technology*, **34**(4): 501—504


## 附中文参考文献


阿布都瓦斯提• 吾拉木. 2006. 基于 *n* 维光谱特征空间的农田干旱遥感监测. 北京大学博士学位论文

李杏朝, 董文敏. 1996. 利用遥感和 GIS 监测旱情的方法研究. 遥感技术与应用, **11**(3): 7—15

齐述华, 王长耀, 牛铮, 刘正军. 2004. 利用 NDVI 时间序列数据分析植被长势对气候因子的响应. 地理科学进展, **23**(3): 91—99

佘万明, 叶彩华. 2006. MODIS 资料遥感监测土壤水分与干旱研究进展. 河南气象, (1): 44—46

宋小宁, 赵英时. 2004. 应用 MODIS 卫星数据提取植被-温度-水分综合指数的研究. 地理与地理信息科学, **20**(2): 13—17

谭德宝, 刘良明, 鄢俊洁, 胡艳. 2004. MODIS 数据的干旱监测模型研究. 长江科学院院报, **21**(3): 11—15

肖乾广, 陈维英, 盛永伟, 李靖. 1994. 用气象卫星监测土壤水分的实验研究. 应用气象学报, **5**(3): 312—318

杨军, 董超华, 卢乃锰, 杨忠东, 施进明, 张鹏, 刘玉洁, 蔡斌. 2009. 中国新一代极轨气象卫星——风云三号. 气象学报, **67**(4): 501—509

詹志明, 秦其明, 阿布都瓦斯提·吾拉木, 汪冬冬. 2006. 基于 NIR-Red 光谱特征空间的土壤水分监测新方法. 中国科学 D 辑, **36**(11): 1020—1026

张文宗, 姚树然, 赵春雷, 王云秀. 2006. 利用 MODIS 资料监测和预警干旱新方法. 气象科技, **34**(4): 501—504